Electronic Supplementary Information (ESI) for

Ba-MOFs with tetrazole-based acetic acids: unusual configuration, novel topology and high proton conductivity

Jie Yang,[a,b†] Shunlin Zhang,[a†] Zhe Feng,[a] Ying Cao,[a] Dun-Ru Zhu[a,c*]
[a] College of Chemical Engineering, State Key Laboratory of Materials-oriented Chemical Engineering, Nanjing Tech University, Nanjing 211816, P.R. China.
[b] College of Materials Engineering, Jiangsu Key Laboratory of Advanced Functional Materials, Changshu Institute of Technology, Changshu 215500, P.R. China
[c] State Key Laboratory of Coordination Chemistry, Nanjing University, Nanjing 210023, P.R. China

Contents

Experimental Section

1. General Remarks

The reagents were obtained from commercial sources and used without further purification. The new ligand H_3L^3 was prepared according to our designed method as shown in Scheme S1. Melting points were determined with an X-4 digital microscope melting-point apparatus (Beijing) and are uncorrected. Elemental analyses (C, H, N) were carried out with a PerkinElmer 240 microanalyzer. ^{1}H NMR spectra in solution

were recorded on a Bruker AM 500 Hz spectrometer. Chemical shifts are given in ppm. IR spectra were recorded in the range 4000-400 cm^{-1} using KBr pellets on a Nicolet 380 FT-IR spectrometer. Powder X-ray diffraction patterns (PXRD) were measured using a Bruker D8 Advance diffractometer. The photoluminescence spectra were recorded on a Hitachi F4600 spectrophotometer. Thermogravimetric analyses (TGA) were performed on a NETZSCH STA 449C thermal analyzer under a N_2 atmosphere at a heating rate of 10°C min^{-1}.

2. Synthesis of H_3L^3 Ligand

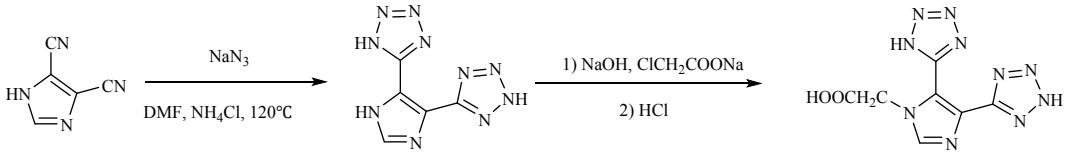

Scheme S1 The synthetic route of 4,5-di(tetrazol-5-yl)imidazolylacetic acid (H_3L^3)

4,5-dicyanoimidazole (11.8096 g, 0.1 mol) and ammonium chloride (16.0474 g, 0.3 mol) were dissolved in 150 mL DMF. Then, sodium azide (19.5030 g, 0.3 mol) was added. The mixture was refluxed at 120°C with stirring for 24 h. After cooled to room temperature, DMF solvent was removed by rotary evaporation, and the reaction solution was adjusted to pH = 10-11 with NaOH and then filtered. The filtrate was adjusted to pH = 2 with HCl, and the 4,5-di(tetrazol-5-yl)imidazole was obtained as a white solid of 14.9651 g, yield 73.3%. FT-IR (KBr, cm^{-1}): 3156, 3014, 2765, 2373, 1633, 1568, 1506, 1403, 1160, 1068, 1007, 885.

After 4,5-di(tetrazol-5-yl)imidazole (4.0831 g, 0.02 mol) was dissolved in 30 mL methanol, $ClCH_2COONa$ (11.6479 g, 0.1 mol) was added, and pH of the solution was adjusted with 1 M NaOH solution to 11, the mixture was refluxed at 100°C under stirring for 48 hours. After cooled to room temperature, methanol solvent was removed by rotary evaporation, the residue was acidified with HCl, and the precipitate was separated by filtration, and washed with water, then dried under vacuum to give the target ligand H_3L^3 in a yield of 84.6%. m.p. 121-123°C. Anal. calcd. for $C_7H_6N_{10}O_2$ (%): C, 32.07; H, 2.31; N, 53.42. Found (%): C, 32.19; H, 2.13; N, 53.24.

FT-IR (KBr, cm^{-1}): 3500, 3002, 1737, 1631, 1579, 1437, 1401, 1343, 1310, 1207, 1062, 1004, 954, 885, 808. ^{1}H NMR (500 MHz, DMSO), 13.38 (1H, s, tetrazolyl-H), 12.99 (1H, s, tetrazolyl-H), 10.28 (1H, s, COOH), 8.00 (1H, s, imidazolyl-H), 5.11 (2H, s, CH_2).

3. Molecular Structures of MOFs 1-3

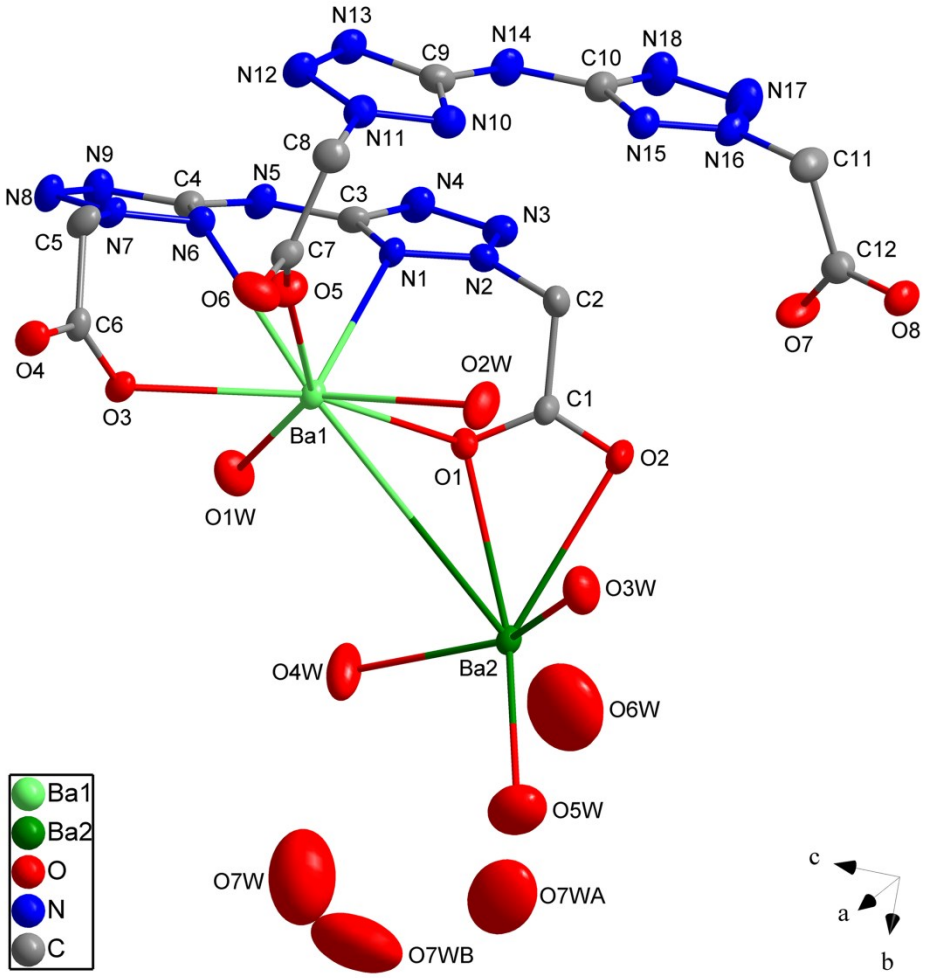

Fig. S1 The asymmetric units of **1**, hydrogen atoms are omitted for clarity.

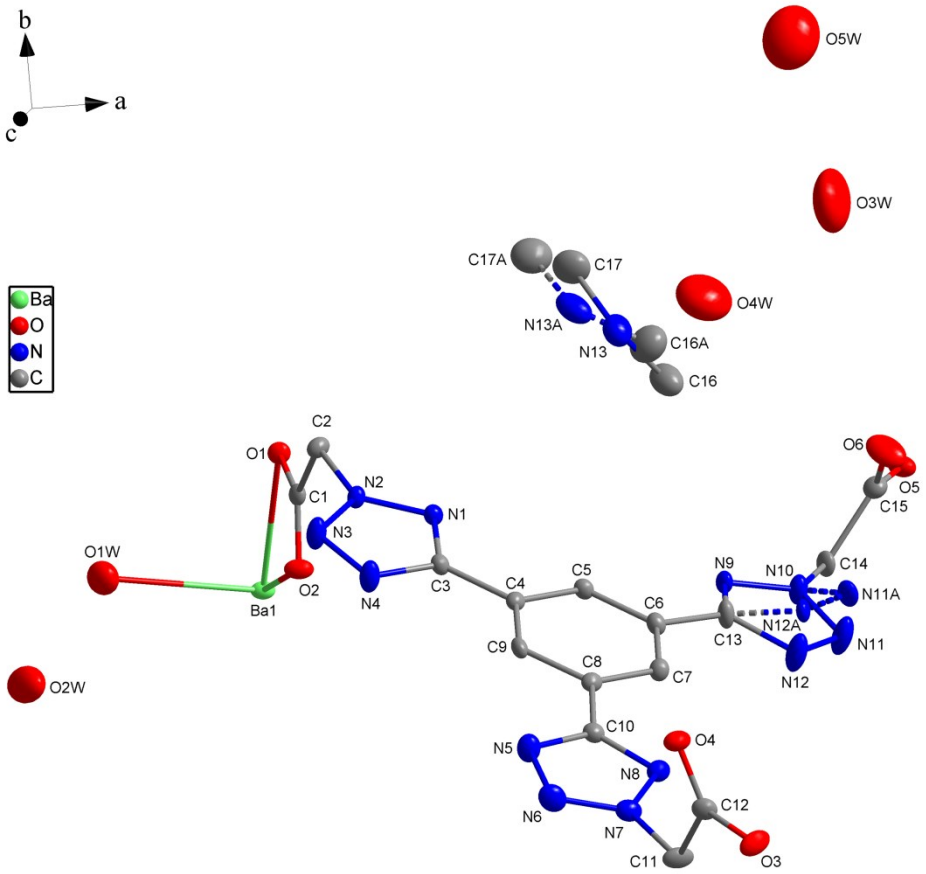

Fig. S2 The asymmetric units of **2**, hydrogen atoms are omitted for clarity.

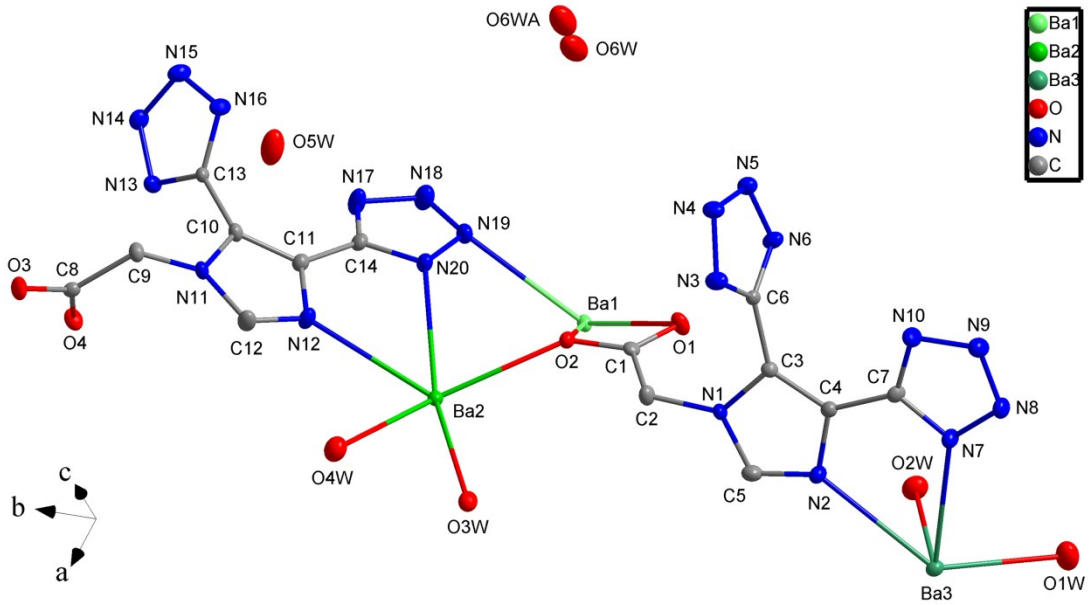

Fig. S3 The asymmetric units of **3**, hydrogen atoms are omitted for clarity.

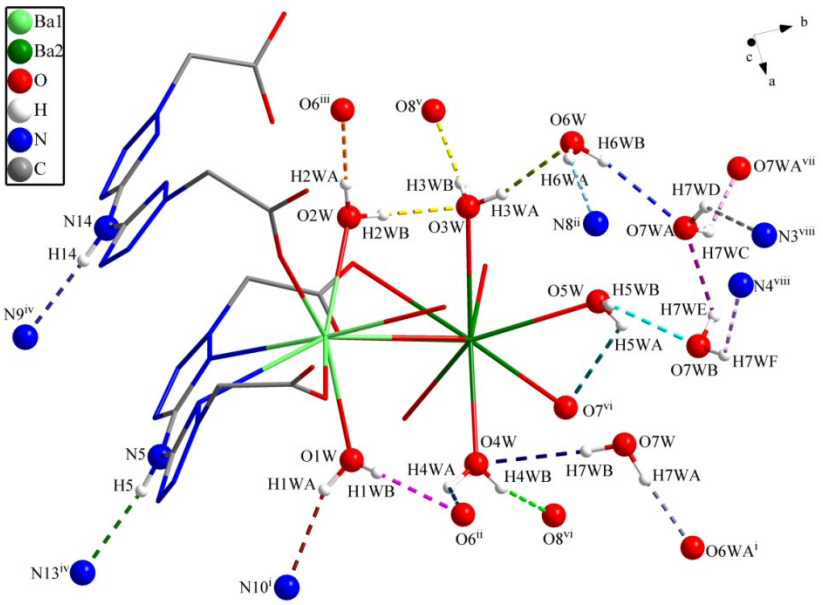

Fig. S4 The hydrogen bond interactions in **1**

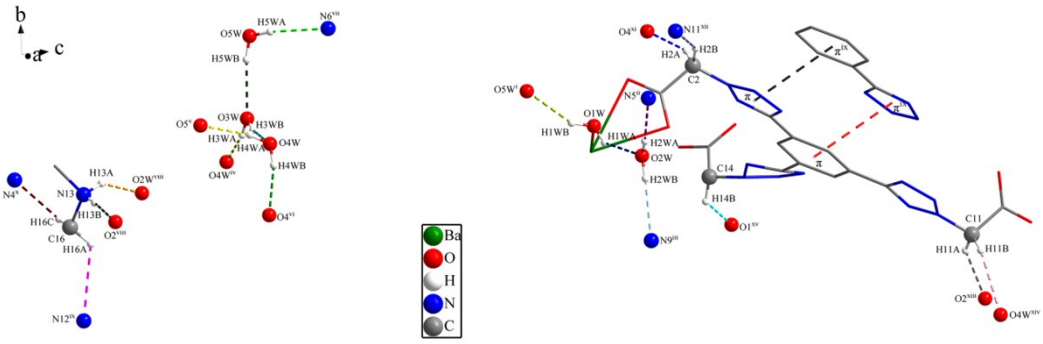

Fig. S5 The hydrogen bonds interactions in **2**

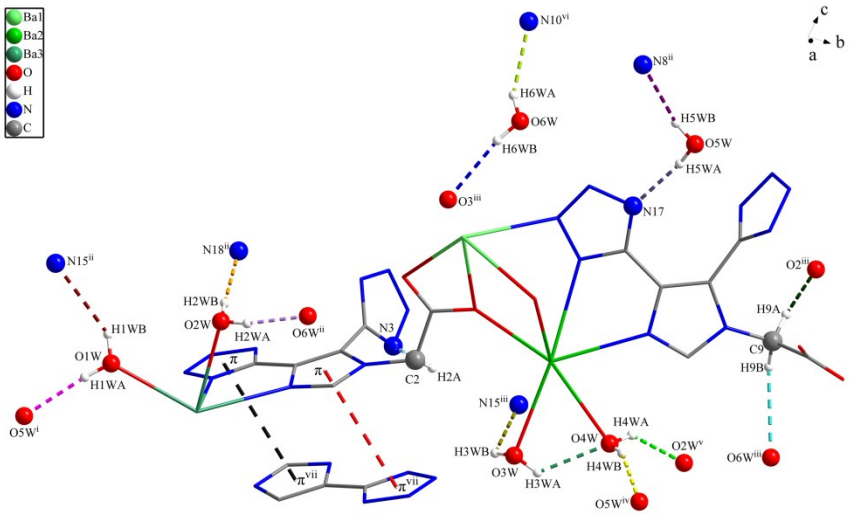

Fig. S6 The hydrogen bond interactions in **3**

4. Tables of Selected Bond Distance and Angles and Weak Interactions for 1-3

Table S1 Selected bond distance (Å) for MOFs **1-3**

			1		
Ba1-O1	2.764(4)	Ba1-O1W	2.710(4)	Ba2-O8^{iii}	2.850(4)
Ba1-O3	2.766(4)	Ba1-O2W	2.750(4)	Ba2-O3W	2.938(5)
Ba1-O3^{i}	2.850(4)	Ba2-O1	2.835(4)	Ba2-O4W	2.751(5)
Ba1-O4^{i}	2.870(4)	Ba2-O2	3.023(5)	Ba2-O5W	2.832(6)
Ba1-O5	2.650(4)	Ba2-O2^{ii}	2.681(4)	Ba1···Ba2	4.6793(18)
Ba1-N1	3.054(5)	Ba2-O4^{i}	2.752(4)	Ba1···Ba1^{i}	4.5173(13)
Ba1-N6	3.106(5)	Ba2-O7^{ii}	2.763(4)	Ba2···Ba2^{ii}	4.7945(14)
			2		
Ba1-O1	2.911(3)	Ba1-O3^{ii}	2.687(3)	Ba1-O5^{iv}	2.831(3)
Ba1-O1^{i}	2.765(3)	Ba1-O3^{iii}	2.804(3)	Ba1-O5^{v}	2.831(3)
Ba1-O1W	2.797(4)	Ba1-O4^{iii}	2.989(3)	Ba1-O6^{v}	3.034(4)
Ba1-O2	2.885(3)	Ba1···Ba1^{vi}	4.284(3)		
			3		
Ba1-O1^{i}	2.766(3)	Ba2-O2	2.760(3)	Ba3-N2	2.883(3)
Ba1-O1	2.939(3)	Ba2-O4^{iii}	2.677(3)	Ba3-N3^{vi}	2.854(4)
Ba1-O2	2.796(3)	Ba2-N4^{iv}	3.182(4)	Ba3-N7	2.933(4)
Ba1-O3^{ii}	2.668(3)	Ba2-N12	2.882(3)	Ba3-N9^{iv}	3.025(4)
Ba1-O3^{iii}	2.863(3)	Ba2-N13^{iii}	2.948(4)	Ba3-N14^{viii}	2.935(3)
Ba1-O4^{iii}	2.860(3)	Ba2-N16^{v}	2.935(3)	Ba3-O1W	2.783(3)
Ba1-N5^{iv}	3.091(4)	Ba2-N20	3.007(4)	Ba3-O2W	2.797(3)
Ba1-N6^{i}	2.942(4)	Ba2-O3W	2.901(3)	Ba3-O3W^{vii}	2.807(3)
Ba1-N19	2.901(4)	Ba2-O4W	2.909(3)	Ba1···Ba1^{ix}	4.554(3)
Ba1···Ba2	4.396(3)	Ba2···Ba3^{vii}	4.950(2)	Ba3···Ba3^{vi}	8.214(2)

Symmetry codes: **1**: i) 1-*x*, 1-*y*, 1-*z*; ii) 1-*x*, 1-*y*, 2-*z*; iii) 1+*x*, *y*, *z*. **2**: (i) 0.5-*x*, *y*-0.5, 1.5-*z*; (ii) 1-*x*, -*y*, 2-*z*; (iii) *x*-0.5, 0.5-*y*, *z*-0.5; (iv) 1-*x*, *y*, 1.5-*z*; (v) *x*-0.5, *y*-0.5, *z*; (vi) 0.5-*x*, 0.5+*y*, 1.5-*z*. **3**: i) 1-*x*, 1-*y*, 1-*z*; ii) *x*, *y*-1, *z*; iii) 2-*x*, 2-*y*, 1-*z*; iv) 1+*x*, *y*, *z*; v) 1-*x*, 2-*y*, 1-*z*; vi) 1-*x*, 1-*y*, -*z*; vii) 2-*x*, 1-*y*, -*z*; viii) *x*, *y*-1, *z*-1; ix) 1-*x*, 1-*y*, 1-*z*.

Table S2 Selected bond angles (°) for MOFs **1-3**

		1	
O1-Ba1-O3	151.50(12)	O2W-Ba1-N6	131.47(14)
O1-Ba1-O3^{i}	110.32(12)	O5-Ba1-O2W	75.19(13)
O1-Ba1-O4^{i}	66.66(12)	O1-Ba2-O8^{iii}	75.23(12)
O1-Ba1-N1	59.81(12)	O2^{ii}-Ba2-O1	109.48(12)
O1-Ba1-N6	112.43(12)	O2-Ba2-O2^{ii}	65.73(15)
O3-Ba1-O3^{i}	72.91(13)	O2^{ii}-Ba2-O4^{i}	143.60(14)
O3-Ba1-O4^{i}	104.69(12)	O2^{ii}-Ba2-O3W	72.97(14)
O3^{i}-Ba1-O4^{i}	45.71(11)	O2^{ii}-Ba2-O4W	143.90(15)
O3^{i}-Ba1-N1	169.57(11)	O4^{i}-Ba2-O1	67.31(12)
O3-Ba1-N1	117.28(12)	O4^{i}-Ba2-O7^{ii}	123.40(15)
O3-Ba1-N6	62.51(12)	O4^{i}-Ba2-O8^{iii}	128.37(12)
O3^{i}-Ba1-N6	134.75(12)	O4^{i}-Ba2-O3W	70.66(14)
O4^{i}-Ba1-N1	125.59(12)	O7^{ii}-Ba2-O1	146.78(13)

O4^{i}-Ba1-N6	153.23(13)	O7^{ii}-Ba2-O2^{ii}	137.62(14)
O5-Ba1-O1	136.30(13)	O7^{ii}-Ba2-O8^{iii}	74.99(14)
O5-Ba1-O3	71.79(13)	O7^{ii} -Ba2-O3W	130.12(14)
O5-Ba1-O4^{i}	123.05(13)	O7^{ii}-Ba2-O5W	63.51(18)
O5-Ba1-N1	102.70(14)	O8-Ba2-O2^{ii}	75.68(13)
O5-Ba1-N6	77.28(13)	O8^{iii}-Ba2-O3W	138.18(14)
O5-Ba1-O1W	147.00(14)	O3W-Ba2-O2	63.83(14)
O1W-Ba1-O1	74.77(13)	O4W-Ba2-O2^{ii}	128.18(16)
O1W-Ba1-O3	76.74(14)	O4W-Ba2-O4^{i}	71.96(15)
O1W-Ba1-O4^{i}	74.34(14)	O4W-Ba2-O7^{ii}	69.18(15)
O1W-Ba1-N6	79.64(14)	O4W-Ba2-O8^{iii}	72.57(16)
O1W-Ba1-O2W	137.54(14)	O4W-Ba2-O3W	142.22(15)
O2W-Ba1-O1	66.95(12)	O5W-Ba2-O1	147.29(16)
O2W-Ba1-O3	139.06(13)	O5W-Ba2-O2	130.94(18)
O2W-Ba1-O3^{i}	79.29(14)	O5W-Ba2-O8^{iii}	137.44(17)
O2W-Ba1-O4^{i}	74.18(14)	O5W-Ba2-O3W	71.80(19)
	2		
O1-Ba1-O1^{i}	138.19(6)	O3^{ii}-Ba1-O4^{iii}	138.31(9)
O1-Ba1-O6^{v}	110.42(9)	O3^{iii}-Ba1-O5^{iv}	70.59(10)
O1^{i}-Ba1-O2	143.25(9)	O3^{ii}-Ba1-O5^{v}	72.27(10)
O1^{i}-Ba1-O4^{iii}	70.69(9)	O3^{ii}-Ba1-O5^{iv}	72.73(10)
O1-Ba1-O4^{iii}	106.59(8)	O3^{iii}-Ba1-O5^{v}	131.53(9)
O1^{i}-Ba1-O5^{v}	66.59(9)	O3^{ii}-Ba1-O6^{v}	74.74(12)
O1^{i}-Ba1-O5^{iv}	74.89(9)	O3^{iii}-Ba1-O6^{v}	143.18(12)
O1^{i}-Ba1-O6^{v}	108.15(9)	O3^{ii}-Ba1-O1W	140.81(12)
O1^{i}-Ba1-O1W	128.83(11)	O4^{iii}-Ba1-O6^{v}	114.08(11)
O2-Ba1-O1	45.23(8)	O5^{iv}-Ba1-O4^{iii}	101.72(9)
O2-Ba1-O4^{iii}	144.81(9)	O5^{iv}-Ba1-O6^{v}	143.14(11)
O2-Ba1-O6^{v}	70.87(9)	O5^{v}-Ba1-O6^{v}	44.07(9)
O3^{ii}-Ba1-O1	107.57(9)	O5^{iv}-Ba1-O1	64.69(9)
O3^{iii}-Ba1-O1	64.45(8)	O5^{iii}-Ba1-O1	154.33(9)
O3^{ii}-Ba1-O1^{i}	67.98(9)	O5^{v}-Ba1-O2	112.72(9)
O3^{iii}-Ba1-O2	109.18(8)	O5^{iv}-Ba1-O5^{v}	135.20(8)
O3^{ii}-Ba1-O2	76.81(9)	O1W-Ba1-O3^{iii}	76.81(12)
O3^{ii}-Ba1-O3^{iii}	142.04(5)	O1W-Ba1-O4^{iii}	67.18(11)
O3^{ii}-Ba1-O4^{iii}	138.31(9)	O1W-Ba1-O5^{iv}	140.85(11)
O3^{iii}-Ba1-O4^{iii}	44.87(8)	O1W-Ba1-O6^{v}	66.42(12)
	3		
O1^{i}-Ba1-O1	74.08(9)	O2-Ba2-N4^{iii}	62.59(9)
O1^{i}-Ba1-O2	107.11(9)	O2-Ba2-N12	123.72(9)
O1^{i}-Ba1-O3^{iii}	140.94(9)	O2-Ba2-N13^{iii}	131.53(9)
O1^{i}-Ba1-O4^{iii}	158.16(8)	O2-Ba2-N16^{v}	73.43(9)
O1-Ba1-N5^{iv}	72.23(9)	O2-Ba2-N20	70.43(9)
O1^{i}-Ba1-N5^{iv}	137.89(9)	O2-Ba2-O4W	142.83(9)
O1-Ba1-N6^{i}	141.57(9)	O4^{iii}-Ba2-O2	76.62(9)
O2-Ba1-O1	45.59(8)	O4^{iii}-Ba2-N13^{iii}	74.71(10)
O2-Ba1-O3^{iii}	111.91(9)	O4^{iii}-Ba2-N16^{v}	143.19(9)

O2-Ba1-O4^{iii}	73.15(8)	O4^{iii}-Ba2-N20	59.66(10)
O2-Ba1-N5^{iv}	63.92(9)	O2-Ba2-N12	123.72(9)
O2-Ba1-N6^{i}	170.84(8)	O4^{iii}-Ba2-O3W	132.52(9)
O2-Ba1-N19	78.18(10)	N2-Ba3-N14^{viii}	130.58(10)
O3^{iii}-Ba1-O1	135.56(9)	N3^{vi}-Ba3-N14^{viii}	70.78(10)
O3^{ii}-Ba1-O2	115.02(9)	N7-Ba3-N9^{iv}	137.49(10)
O3^{ii}-Ba1-O3^{iii}	79.04(9)	N14^{viii}-Ba3-N9^{iv}	137.89(10)
O3^{ii}-Ba1-O4^{iii}	116.80(9)	O1W-Ba3-N2	134.96(10)
O3^{iii}-Ba1-N5^{iv}	63.47(9)	O1W-Ba3-N3^{vi}	136.83(10)
O3^{ii}-Ba1-N5^{iv}	67.01(10)	O1W-Ba3-N9^{iv}	115.96(11)
O3^{ii}-Ba1-N6^{i}	74.02(10)	O1W-Ba3-N14^{viii}	67.54(10)
O3^{iii}-Ba1-N6^{i}	67.18(10)	O1W-Ba3-O2W	74.78(10)
O3^{ii}-Ba1-N19	166.80(10)	O2W-Ba3-N2	70.91(10)
O4^{iii}-Ba1-O1	115.41(8)	O2W-Ba3-N3^{vi}	148.29(10)
O4^{iii}-Ba1-O3^{iii}	45.56(8)	O2W-Ba3-N9^{iv}	70.86(11)
O4^{iii}-Ba1-N5^{iv}	62.69(9)	O2W-Ba3-N14^{viii}	140.21(10)
O4^{iii}-Ba1-N6^{i}	101.85(9)	O2W-Ba3-O3W^{vii}	109.45(10)
O4^{iii}-Ba1-N19	65.36(9)	O3W^{vii}-Ba3-N2	142.59(9)
N6^{i}-Ba1-N5^{iv}	121.11(9)	O3W^{vii}-Ba3-N7	154.58(9)
N19-Ba1-O1	110.49(10)	O3W^{vii}-Ba3-N9^{iv}	66.88(9)
N19-Ba1-N5^{iv}	122.03(10)	O3W^{vii}-Ba3-N14^{viii}	74.18(9)

Symmetry codes: **1**: i) 1-*x*, 1-*y*, 1-*z*; ii) 1-*x*, 1-*y*, 2-*z*; iii) 1+*x*, *y*, *z*; **2**: (i) 0.5-*x*, -0.5-*y*, 1.5-*z*; (ii) 1-*x*, -*y*, 2-*z*; (iii) *x*-0.5, 0.5-*y*, *z*-0.5; (iv) 1-*x*, *y*, 1.5-*z*; (v) *x*-0.5, *y*-0.5, *z*; **3**: i) 1-*x*, -*y*, 1-*z*; ii) *x*, *y*-1, *z*; iii) 2-*x*, 2-*y*, 1-*z*; iv) 1+*x*, *y*, *z*; v) 1-*x*, 2-*y*, 1-*z*; vi) 1-*x*, 1-*y*, -*z*; vii) 2-*x*, 1-*y*, -*z*; viii) *x*, *y*-1, *z*-1.

Table S3 Hydrogen-bond geometry (Å, °) in **1-3**

D–H···A	*d*(D–H)	*d*(H···A)	*d*(D···A)	∠D–H···A
		1		
O1W–H1WA···N10^{i}	0.85	2.29	3.028(4)	146
O1W–H1WB···O6^{ii}	0.85	2.01	2.735(4)	142
O2W–H2WA···O6^{iii}	0.85	1.86	2.710(4)	178
O2W–H2WB···O3W	0.85	2.11	2.964(4)	179
N5–H5···N13^{iv}	0.86	2.12	2.952(4)	164
O3W–H3WA···O6W	0.85	2.06	2.897(4)	166
O3W–H3WB···O8^{v}	0.85	2.05	2.882(4)	165
O4W–H4WA···O6^{ii}	0.85	2.59	3.111(3)	121
O4W–H4WB···O8^{vi}	0.85	2.10	2.897(3)	156
O5W–H5WA···O7^{vi}	0.85	2.48	2.944(3)	116
O5W–H5WB···O7WB	0.85	2.29	2.951(3)	135
O6W–H6WA···N8^{ii}	0.85	2.39	3.197(4)	158
O6W–H6WB···O7WA	0.85	2.21	3.000(4)	155
O7WA–H7WC···O7WA^{vii}	0.85	1.74	2.340(4)	126
O7WA–H7WD···N3^{viii}	0.85	2.48	3.137(4)	134
O7WB–H7WE···O7WA	0.85	1.94	2.558(3)	129

O7WB–H7WF···N4^{viii}	0.85	2.55	3.113(5)	124
O7W–H7WA···O6W^{i}	0.85	1.74	2.584(4)	176
O7W–H7WB···O4WB	0.85	2.44	3.289(3)	177
N14-H14···N9^{iv}	0.86	2.02	2.874(3)	171
		2		
O1W–H1WA···O2W	0.85	2.04	2.797(2)	149
O1W–H1WB···O5W^{i}	0.85	2.31	3.084(3)	152
O2W–H2WA···N5^{ii}	0.85	2.01	2.851(3)	167
O2W–H2WB···N9^{iii}	0.85	2.21	3.047(2)	168
O3W–H3WA···O4W^{iv}	0.85	2.05	2.878(2)	165
O3W–H3WB···O4W	0.85	2.05	2.878(2)	165
O4W–H4WA···O5^{V}	0.85	2.07	2.903(3)	165
O4W–H4WB···O4^{vi}	0.85	2.12	2.942(3)	164
O5W–H5WA···N6^{vii}	0.85	2.31	3.157(2)	172
O5W–H5WB···O3W	0.85	2.08	2.924(3)	172
N13–H13A···O2W^{viii}	0.90	2.34	3.104(3)	143
N13–H13B···O2^{viii}	0.90	1.97	2.871(3)	176
C16–H16A···N12^{ix}	0.96	2.72	3.348(2)	123
C16–H16C···N4^{x}	0.96	2.55	3.446(3)	155
C2–H2A···O4^{xi}	0.97	2.34	3.241(3)	155
C2–H2B···N11^{xii}	0.97	2.47	3.331(3)	147
C11–H11A···O2^{xiii}	0.97	2.46	3.332(3)	149
C11–H11B···O4W^{xiv}	0.97	2.54	3.419(2)	151
C14–H14B···O1^{xv}	0.97	2.66	3.410(3)	135
		3		
O1W–H1WA···O5W^{i}	0.85	2.03	2.880(4)	174
O1W–H1WB···N15^{ii}	0.85	2.49	3.232(5)	146
O2W–H2WA···O6W^{ii}	0.85	1.90	2.736(4)	169
O2W–H2WB···N18^{ii}	0.85	2.07	2.916(4)	171
O3W–H3WA···O4W	0.85	2.20	2.714(4)	119
O3W–H3WB···N15^{iii}	0.85	2.66	3.184(5)	121
O4W–H4WA···O5W^{iv}	0.85	2.00	2.794(5)	155
O4W–H4WB···O2W^{v}	0.85	2.20	2.921(4)	143
O5W–H5WA···N17	0.85	1.93	2.766(4)	166
O5W–H5WB···N8^{ii}	0.85	2.26	3.074(5)	162
O6W–H6WA···N10^{vi}	0.85	2.17	2.936(4)	150
O6W–H6WB···O3^{iii}	0.85	2.28	3.110(5)	166
C2–H2A···N3	0.97	2.90	3.494(5)	121
C9–H9A···O2^{iii}	0.97	2.28	3.215(4)	161
C9–H9B···O6W^{iii}	0.97	2.60	3.287(4)	128

Symmetry codes: **1**: i) 1+*x*, *y*, *z*; ii) 1–*x*, 1–*y*, 2–*z*; iii) –*x*, 1–*y*, 2–*z*; iv) 1–*x*, –*y*, 2–*z*; v) –*x*, 1–*y*, 1–*z*; vi) 1–*x*, 1–*y*, 1–*z*; vii) 1-*x*, 2-*y*, 1-*z*; viii) *x*, 1+*y*, *z*. **2**: i) 0.5–*x*, 1.5–*y*, 1–*z*; ii) 0.5–*x*, 0.5–*y*, 2–*z*; iii) *x*–0.5, *y*–0.5, *z*; iv) 1–*x*, *y*, 0.5–*z*; v) 1–*x*, 1–*y*, 1–*z*; vi) 1–*x*, *y*, 1.5–*z*; vii) 1–*x*, 1+*y*, 1.5–*z*; viii) 0.5–*x*, 0.5–*y*, 1–*z*; ix) 1–*x*, –*y*, 1–*z*; x) *x*, *y*, *z*–1; xi) 1–*x*, 1– *y*, 2–*z*; xii) *x*–0.5, 0.5+*y*, *z*; xiii) 1–*x*, –*y*, 2–*z*; xiv) 1–*x*, *y*–1, 1.5–*z*; xv) 0.5+*x*, *y*–0.5, *z*. **3**: i) *x*, *y*–1, *z*–1; ii) 1–*x*, 1–*y*, 1–*z*; iii) 1–*x*, 2–*y*, 1–*z*; iv) 2–*x*, 2–*y*, 1–*z*; v) *x*, 1+*y*, *z*; vi) –*x*, 1–*y*, 1–*z*.

Table S4 $\pi\cdots\pi$ interactions (Å, °) for the MOFs **2** and **3**

MOFs	$\pi\cdots\pi$ interaction	cent···cent (Å)	dihedral angle (°)
2	π(tez)···π(Ph)^{ix}	3.951	4.7(2)
	π(Ph)···π(tez)^{ix}	3.951	4.7(4)
3	π(im)···π(tez)^{vii}	3.852	7.2(2)
	π(tez)···π(im)^{vii}	3.852	7.2(3)

Symmetry codes: **2**: ix) 1–*x*, –*y*, 1–*z*; **3**: vii) 1–*x*, 1–*y*, –*z*.

Table S5 Dihedral angles (°) of the ligands in MOFs **1-3**

MOFs	Tez/Tez[a]	Ph[b]/Tez	Im[c]/Tez
H_2L^1	9.98(2) (C3/C4-Tez) 6.80(2) (C9/C10-Tez)		
H_3L^2		4.7(1) (C3-Tez) 3.6(5) (C10-Tez) 7.7(4) (C13-Tez)	
H_3L^3			71.8(6) (C13-Tez) 18.7(9) (C14-Tez)

[a]Tez: Tetrazole ring; [b]Ph: Phenyl ring; [c]Im: Imidazole ring

5. The FT-IR Spectra of MOFs 1-3

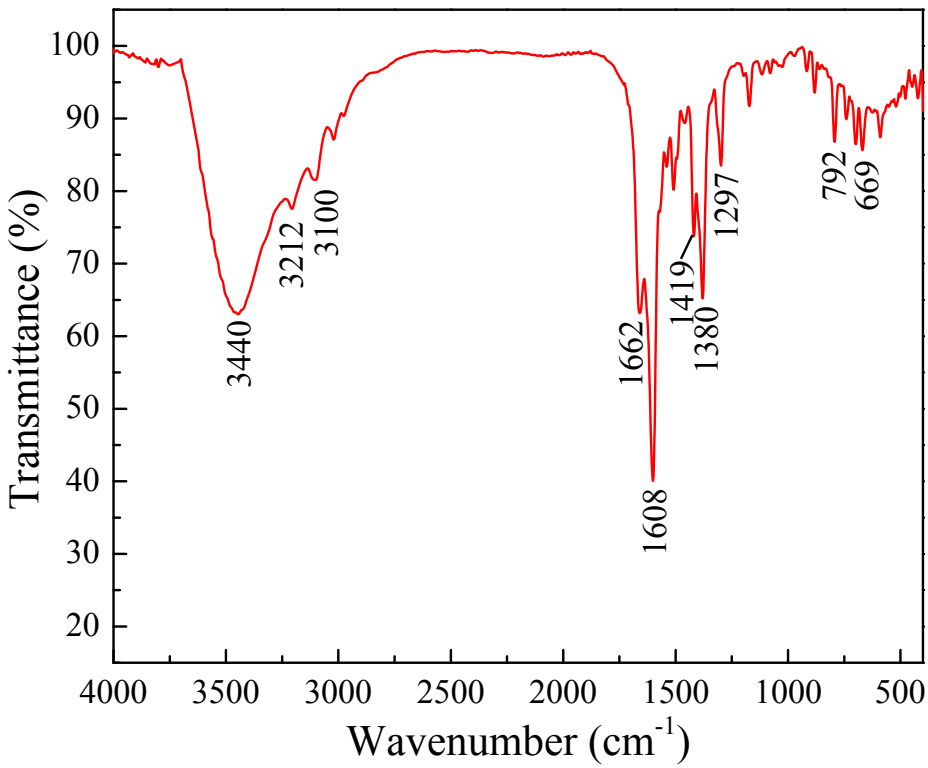

Fig. S7 The IR spectrum of **1**.

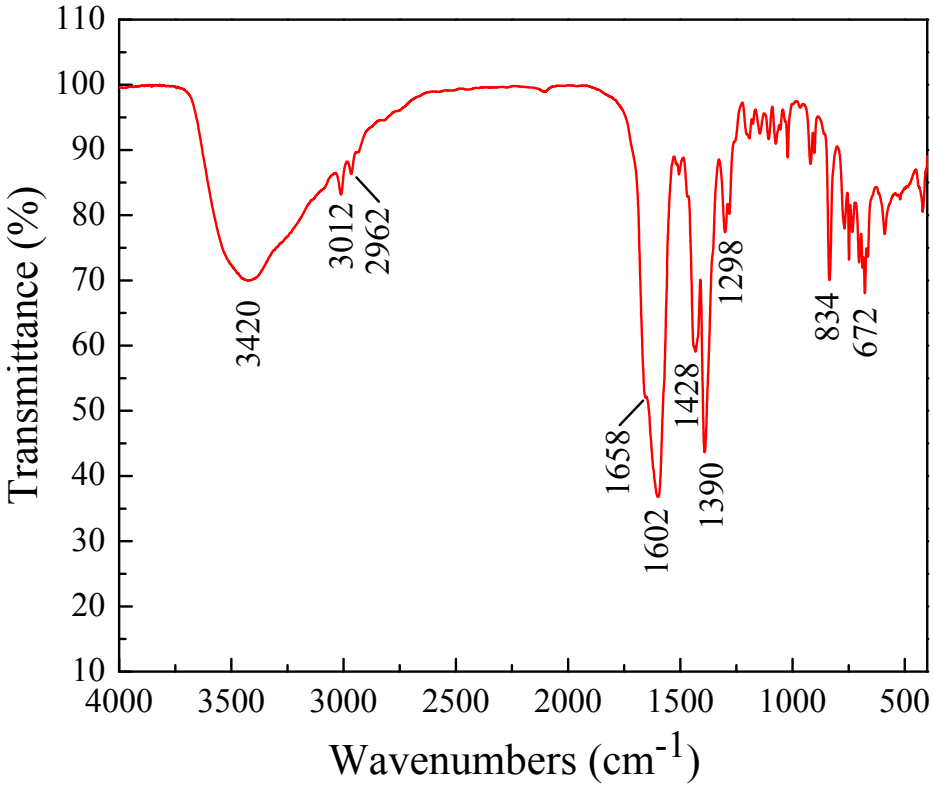

Fig. S8 The IR spectrum of **2**.

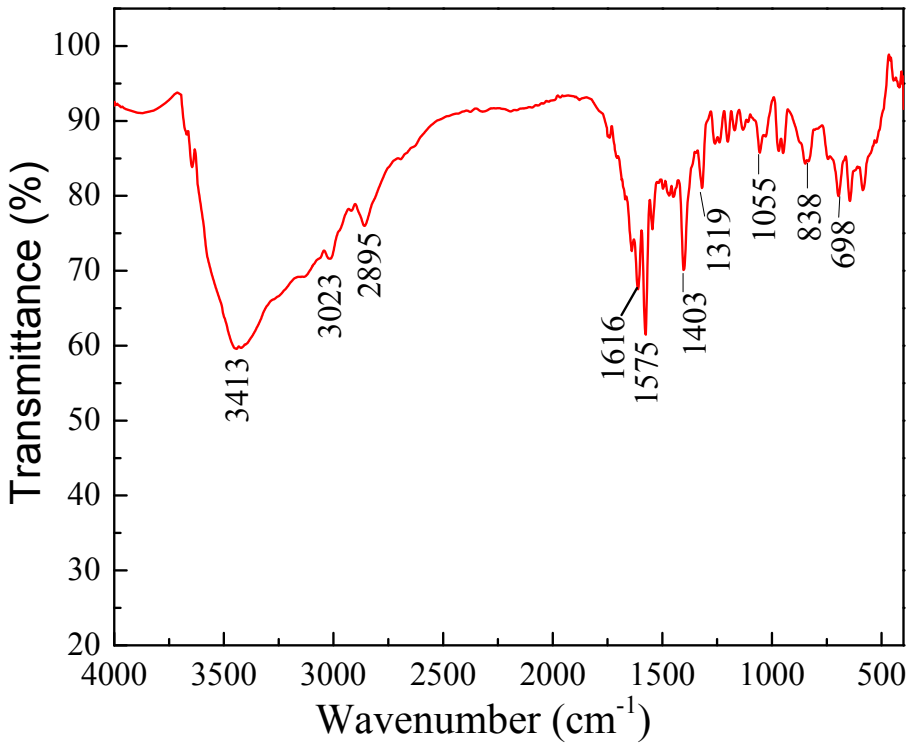

Fig. S9 The IR spectrum of **3**.

6. The PXRD Patterns of MOFs 1-3

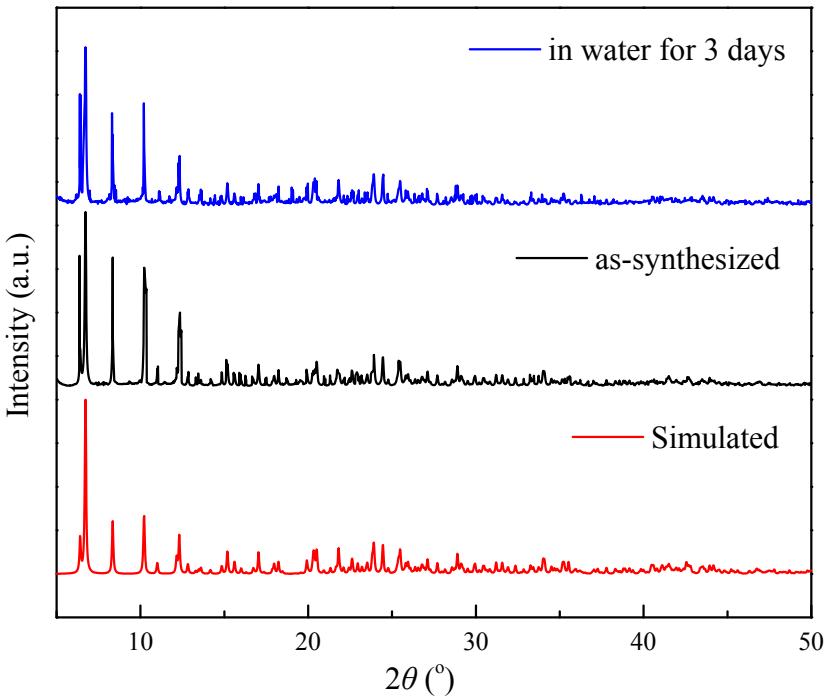

Fig. S10 The PXRD patterns of **1**.

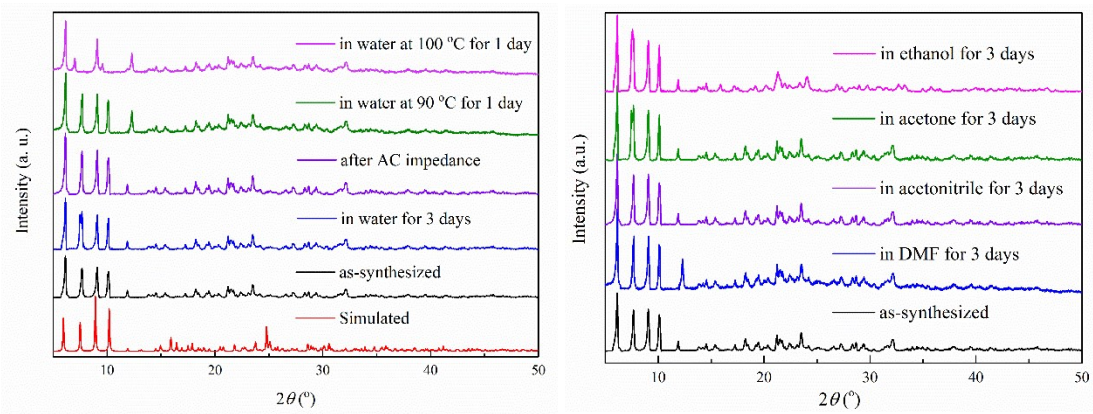

(a) (b)

Fig. S11 The PXRD patterns of **2** in water (a) and different organic solvents (b) compared to the as-synthesized sample.

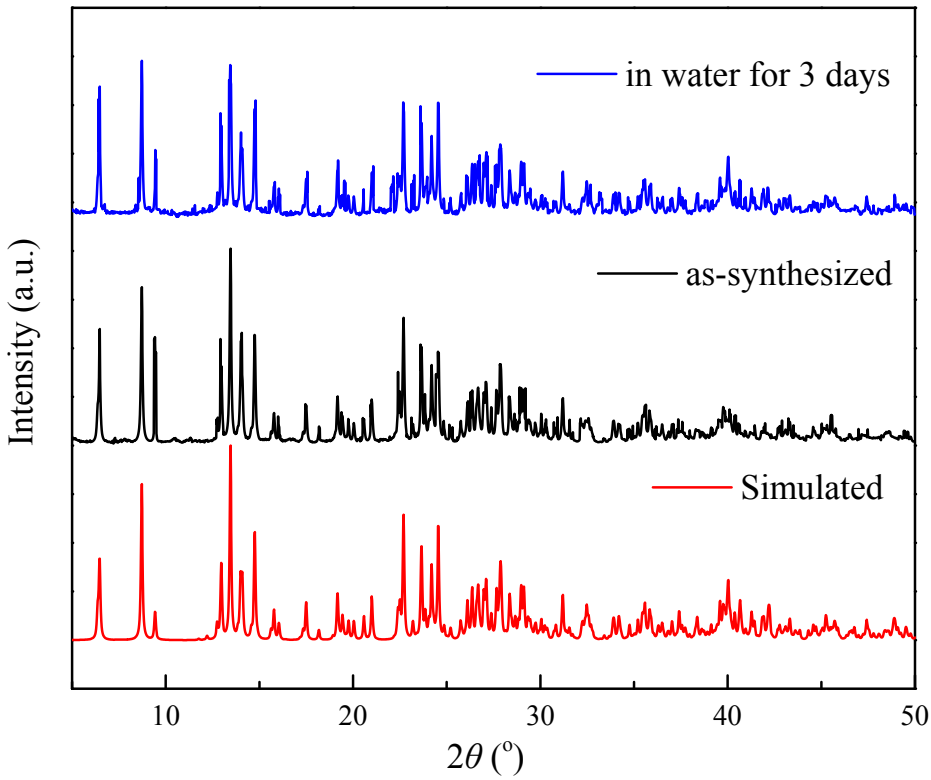

Fig. S12 The PXRD patterns of **3**.

7. The Thermogravimetric Analyses of MOFs 1-3

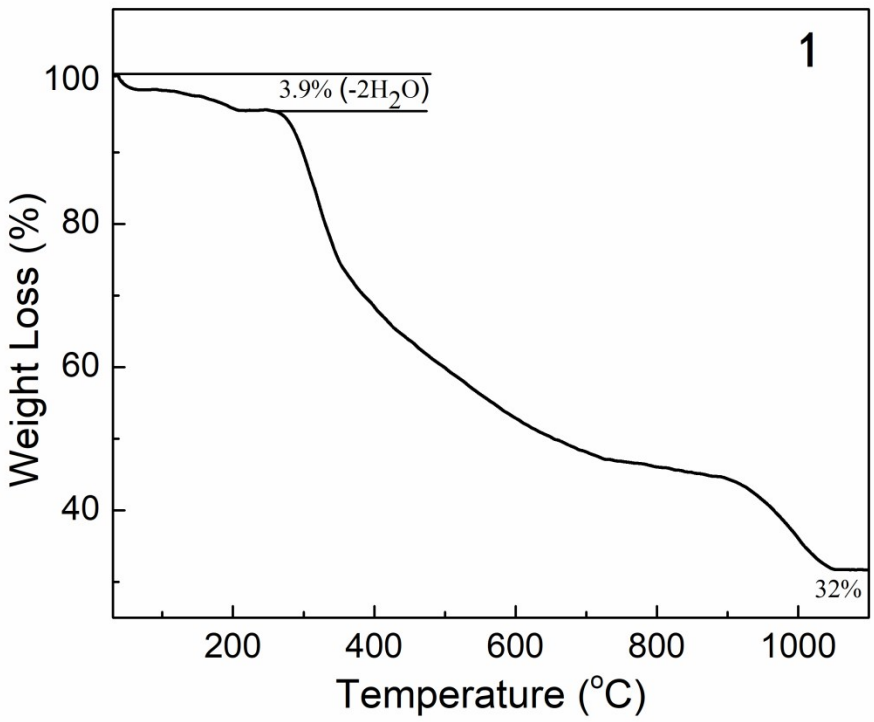

Fig. S13 Thermogravimetric analysis curve of **1**.

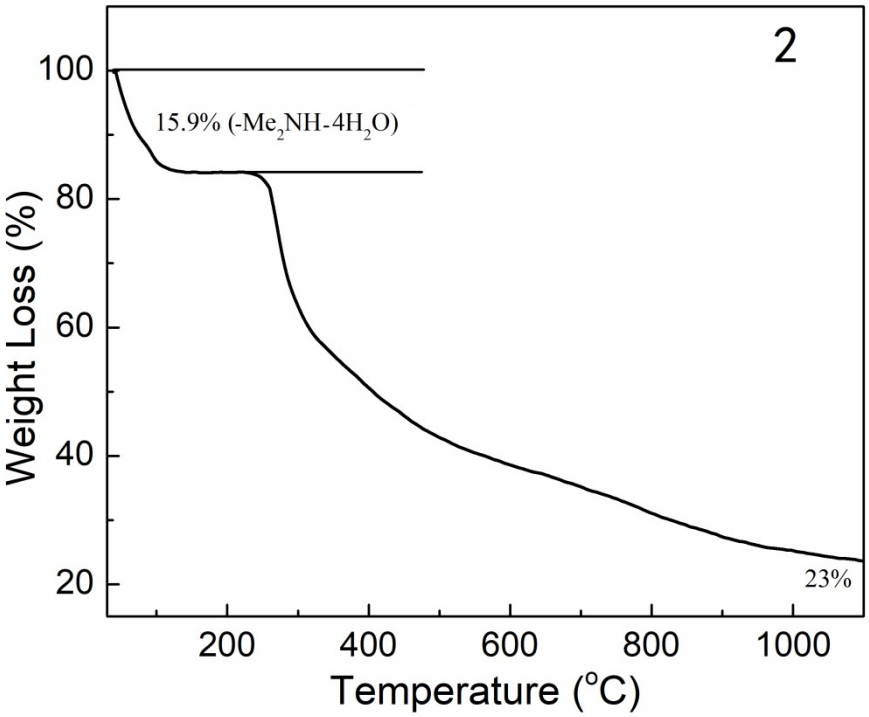

Fig. S14 Thermogravimetric analysis curve of **2**.

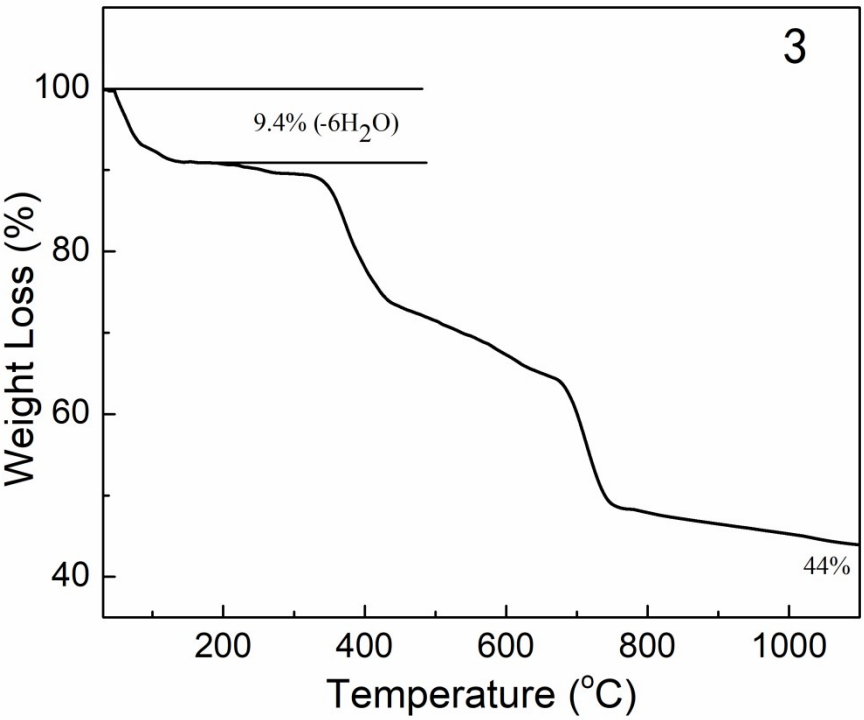

Fig. S15 Thermogravimetric analysis curve of **3**.

8. Luminescence Spectra

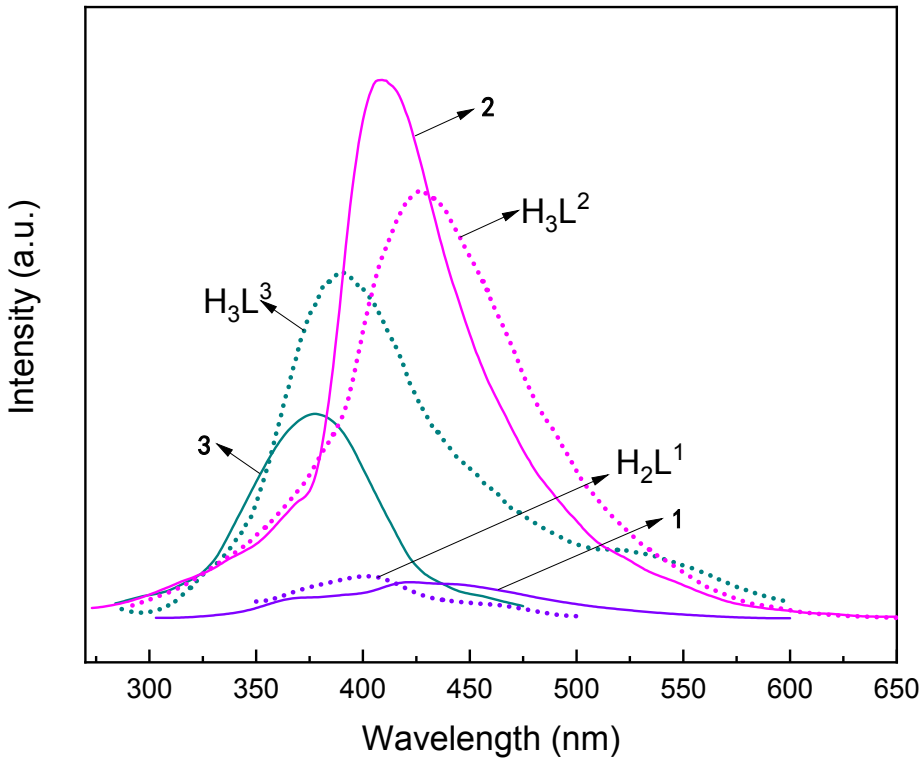

Fig. S16 Solid state emission spectra of the free ligands H_2L^1, H_3L^2, H_3L^3 and MOFs **1**, **2**, **3** at room temperature

9. Proton Conductivity Measurement

The resistance value was determined from equivalent circuit fits of the first semi-circle using ZView Software.

Proton conductivity was calculated using the following equation:

$$\sigma = \frac{l}{SR} \qquad (1)$$

where l and S are the length (cm) and cross-sectional area (cm^2) of the samples respectively, and R, which was extracted directly from the impedance plots, is the bulk resistance of the sample (Ω). Activation energy (E_a) for the materials conductivity was estimated from the following equation:

$$\sigma T = \sigma_0 \exp\left(-\frac{E_a}{k_B T}\right) \qquad (2)$$

where σ is the proton conductivity, σ_0 is the preexponential factor, k_B is the Boltzmann constant, and T is the temperature.

Table S6 Proton conductivities at 25°C with different relative humidity and at 98% relative humidity with different temperature

25°C		98% RH	
RH (%)	σ (S cm^{-1})	T (°C)	σ (S cm^{-1})
50	1.90×10^{-6}	35	2.93×10^{-4}
60	4.56×10^{-6}	45	6.77×10^{-4}
70	1.21×10^{-5}	55	9.32×10^{-4}
80	3.25×10^{-5}	65	1.40×10^{-3}
90	1.03×10^{-4}	75	2.49×10^{-3}
98	1.72×10^{-4}	85	4.47×10^{-3}

Table S7 Proton conductivities of representative MOFs materials above 90% RH

MOFs	Conductivity (S cm^{-1})	Condition	Ref.
H_2SO_4@MIL-101-SO_3H	1.82	70°C 90% RH	1
BUT-8(Cr)A	1.27×10^{-1}	80°C 100% RH	2
UiO-66$(SO_3H)_2$	8.4×10^{-2}	80°C 90% RH	3
$\{H[(N(CH_3)_4)_2][Gd_3(NIPA)_6]\}\cdot 3H_2O$	7.17×10^{-2}	75°C 98% RH	4
Im@MOF-808	3.45×10^{-2}	65°C 99% RH	5
PCMOF-$2_{1/2}$	2.1×10^{-2}	85°C 90% RH	6
PCMOF20	1.3×10^{-2}	85°C 95% RH	7
PCC-72	1.2×10^{-2}	95°C 95% RH	8
MIP-202(Zr)	1.1×10^{-2}	88°C 95% RH	9
JLU-Liu44	8.4×10^{-3}	27°C 98% RH	10
$[Zn(L)Cl]_n$	4.73×10^{-3}	100°C 98% RH	11
Co-MOF-74	4.5×10^{-3}	90°C 95% RH	12
$(Me_2NH_2)[Ba(L^2)(H_2O)]\cdot 3H_2O$	4.47×10^{-3}	85°C 98% RH	This work
$(Me_2NH_2)[In(EBTC)]\cdot DMF\cdot 5H_2O$	3.49×10^{-3}	25°C 99% RH	13
$(N_2H_5)[CeEu(C_2O_4)_4(N_2H_5)]\cdot 4H_2O$	3.42×10^{-3}	25°C 100% RH	14
MFM-512	2.9×10^{-3}	25°C 99% RH	15
$[Me_2NH_2][Eu(ox)_2(H_2O)]\cdot 3H_2O$	2.73×10^{-3}	55°C 95% RH	16
UiO-66(Zr)-(CO_2H)	2.3×10^{-3}	90°C 95% RH	17
JUC-200	1.62×10^{-3}	80°C 98% RH	18

References

1. X.-M. Li, L.-Z. Dong, S.-L. Li, G. Xu, J. Liu, F.-M. Zhang, L.-S. Lu, Y.-Q. Lan, Synergistic conductivity effect in a proton sources-coupled metal-organic framework. *ACS Energy Lett.* 2017, 2313-2318.
2. F. Yang, G. Xu, Y. Dou, B. Wang, H. Zhang, H. Wu, W. Zhou, J.-R. Li, B. Chen, A flexible metal-organic framework with a high density of sulfonic acid sites for proton conduction. *Nat. Energy* 2017, **2**, 877-883.
3. W. J. Phang, H. Jo, W. R. Lee, J. H. Song, K. Yoo, B. Kim, C. S. Hong, Superprotonic conductivity of a UiO-66 framework functionalized with sulfonic acid groups by facile postsynthetic oxidation. *Angew. Chem. Int. Ed.* 2015, **54**, 5142-5146.

4. X. S. Xing, Z. H. Fu, N. N. Zhang, X. Q. Yu, M. S. Wang, G. C. Guo, High proton conduction in an excellent water-stable gadolinium metal-organic framework. *Chem. Commun.*, 2019, **55**, 1241-1244.
5. H.-B. Luo, Q. Ren, P. Wang, J. Zhang, L. Wang, X.-M. Ren, High Proton Conductivity Achieved by Encapsulation of Imidazole Molecules into Proton-Conducting MOF-808. *ACS Appl. Mater. Interfaces*, 2019, **11**, 9164-9171.
6. S. Kim, K. W. Dawson, B. S. Gelfand, J. M. Taylor, G. K. H. Shimizu, Enhancing Proton Conduction in a Metal-Organic Framework by Isomorphous Ligand Replacement. *J. Am. Chem. Soc.*, 2013, **135**, 963-966.
7. Z. H. Fard, N. E. Wong, C. D. Malliakas, P. Ramaswamy, J. M. Taylor, K. Otsubo, G. K. H. Shimizu, Superprotonic Phase Change to a Robust Phosphonate Metal-Organic Framework. *Chem. Mater.*, 2018, **30**, 314-318.
8. L. Qin, Y. Z. Yu, P. Q. Liao, W. Xue, Z. Zheng, X. M. Chen, Y. Z. Zheng, A "Molecular Water Pipe": A Giant Tubular Cluster {Dy72} Exhibits Fast Proton Transport and Slow Magnetic Relaxation. *Adv. Mater.*, 2016, **28**, 10772-10779.
9. S. Wang, M. Wahiduzzaman, L. Davis, A. Tissot, W. Shepard, J. Marrot, C. Martineau-Corcos, D. Hamdane, G. Maurin, S. Devautour-Vinot, C. Serre, A robust zirconium amino acid metal-organic framework for proton conduction. *Nat. Commun.*, 2018, **9**, 49373.
10. L. Zou, S. Yao, J. Zhao, D.-S. Li, G. Li, Q. Huo, Y. Liu, Enhancing Proton Conductivity in a 3D Metal-Organic Framework by the Cooperation of Guest $[Me_2NH_2]^+$ Cations, Water Molecules, and Host Carboxylates. *Cryst. Growth Des.*, 2017, **17**, 3556-3561.
11. Z.-Q. Shi, N.-N. Ji, M.-H. Wang, G. Li, A Comparative Study of Proton Conduction Between a 2D Zinc(II) MOF and Its Corresponding Organic Ligand. *Inorg. Chem.*, 2020, **59**, 4781-4789.
12. S. Hwang, E. J. Lee, D. Song, N. C. Jeong, High Proton Mobility with High Directionality in Isolated Channels of MOF-74. *ACS Appl. Mater. Interfaces*, 2018, **10**, 35354-35360.
13. L. Zhai, J.-W. Yu, J. Zhang, W.-W. Zhang, L. Wang, X.-M. Ren, High quantum yield pure blue emission and fast proton conduction from an indium-metal-organic framework. *Dalton Trans.*, 2019, **48**, 12088-12095.
14. K. Zhang, X. Xie, H. Li, J. Gao, L. Nie, Y. Pan, J. Xie, D. Tian, W. Liu, Q. Fan, H. Su, L. Huang, W. Huang, Highly Water-Stable Lanthanide-Oxalate MOFs with Remarkable Proton Conductivity and Tunable Luminescence. *Adv. Mater.*, 2017, **29**, 1701804.
15. P. Rought, C. Marsh, S. Pili, I. P. Silverwood, V. G. Sakai, M. Li, M. S. Brown, S. P. Argent, I. Vitorica-Yrezabal, G. Whitehead, M. R. Warren, S. Yang, M. Schröder, Modulating proton diffusion and conductivity in metal-organic frameworks by incorporation of accessible free carboxylic acid groups. *Chem. Sci.*, 2019, **10**, 1492-1499.
16. X. Wang, T. Qin, S.-S. Bao, Y.-C. Zhang, X. Shen, L.-M. Zheng, D. Zhu, Facile synthesis of a water stable 3D Eu-MOF showing high proton conductivity and its application as a sensitive luminescent sensor for Cu^{2+} ions. *J. Mater. Chem. A*, 2016, **4**, 16484-16489.
17. D. D. Borges, S. Devautour-Vinot, H. Jobic, J. Ollivier, F. Nouar, R. Semino, T. Devic, C. Serre, F. Paesani, G. Maurin, Proton Transport in a Highly Conductive Porous Zirconium-Based Metal-Organic Framework: Molecular Insight. *Angew. Chem. Int. Ed.*, 2016, **55**, 3919-3924.
18. K. Cai, F. Sun, X. Liang, C. Liu, N. Zhao, X. Zou, G. Zhu, An acid-stable hexaphosphate ester based metal-organic framework and its polymer composite as proton exchange membrane. *J.*

Mater. Chem. A, 2017, **5**, 12943-12950.